



EXPERIMENTAL STUDY ON BRIDGE ABUTMENT BEHAVIOR UNDER EARTHQUAKE-INDUCED LATERAL MOVEMENT OF SOFT CLAY GROUND

Y. Yang⁽¹⁾, S. Tanimoto⁽²⁾, and T. Kiriya⁽³⁾

⁽¹⁾ Research Specialist, Public Works Research Institute, y-yang55@pwri.go.jp

⁽²⁾ Senior Researcher, Public Works Research Institute, s-tanimo@pwri.go.jp

⁽³⁾ Research Coordinator for Earthquake Engineering, Public Works Research Institute, kiriya-t673bs@pwri.go.jp

Abstract

In this study, a dynamic centrifuge experiment is designed to investigate the seismic behavior of an existing bridge subjected to the earthquake-induced lateral movement of a soft clay layer. The pile-supported bridge abutment at the movable bearing side is modeled at the 1/75 scale. The material and thickness of the soft clay layer are set as the experimental parameters. Under the effect of the lateral movement of the soft clay layer during base shaking, a collision between the bridge abutment wall and the girder occurs, and the bridge abutment wall is restrained at the top; however, the footing largely moves forward, resulting in the large backward inclination of the bridge abutment wall. In addition, it is confirmed that during base shaking, the pile bending moment largely increases due to the ground lateral movement and almost remains even at the end of the base shaking phase. Furthermore, it is found that when the material of the soft clay layer has a high shear strength, the ground lateral movement possibly causes a large external earth pressure acting on the piles, resulting in the large corresponding internal bending moment on the pile sections; however, when the soft clay layer has a large thickness, the pile earth pressure largely occurs at only the local position, instead of the whole pile length.

Keywords: Bridge abutment, soft clay, lateral movement, seismic behavior, dynamic centrifuge experiment



1. Introduction

Post-earthquake damage reconnaissance and investigation indicate that in addition to the most well-known ground failure due to liquefaction, the soft clay ground can also be expected to fail during earthquakes and can cause potential damage to bridge structures. Under strong earthquake motions, the lateral movement of the soft clay deposit may lead to the destructive damage to bridge structures as ground liquefaction. For existing bridges designed with old standards, the considered seismic load is generally small, and the gap between the abutment wall and superstructure is always narrow. Under the lateral movement of the soft clay layer during an earthquake, the bridge abutment is expected to move forward. It is possible to raise the collision between the abutment wall and superstructure, but its effect has not been considered in bridge design. The corresponding external and inner force distributions of both the bridge abutment and the superstructure may be largely different from those assumed in the design stage. Consequently, unexpected bridge damage may occur and impede the relief activities after an earthquake in some severe cases. Due to the lateral movement of the thick soft clay layer, the pile foundation damage of existing bridge was also observed in the 2011 off the pacific coast of Tohoku Earthquake of Japan [1]. Thus, to accurately evaluate the seismic performance of the existing bridges constructed on the soft clay deposits, especially with a small gap between the abutment wall and superstructure, it is necessary to consider the effect of the ground lateral movement.

Liquefaction has received much attention in previous studies, and considerable research studies have been conducted to investigate the liquefaction effect on the seismic performance of structures. However, relatively little attention has been paid to the seismic performance of structures constructed on the soft clay deposit. For example, with regard to the seismic behavior evaluation of the soft clay deposits and the pile foundations, the results of two-way cyclic lateral load tests carried out on model pile groups embedded in soft marine clay was reported and discussed [2]. The seismic effects on fixed-head, end-bearing piles installed through soft clay were examined using centrifuge and numerical modelling [3]. Other previous studies related to the dynamic response of pile foundation embedded in soft ground can be found in the references [4-9]. However, in most of these centrifuge tests and the shaking table tests related to the seismic behavior of pile foundation embedded in soft ground, only the single pile or pile groups are modeled and the superstructure is always ignored or simply modeled as a mass block. The reference [10] indicates that not only the bridge foundation but also the bridge superstructure can exert a significant restraining effect on lateral ground deformations, based on the related numerical analysis. In other words, to understand the seismic behavior of bridge, it is necessary to properly consider the superstructure effect.

This research aims to develop an evaluation method for the seismic performance of existing bridges located on the soft clay deposits, which are potentially subjected to the lateral movements during earthquakes. As the first step, to provide basic knowledge for this research, a dynamic centrifuge experiment is designed to investigate the seismic behavior of bridge abutments subjected to earthquake-induced lateral movement of the soft clay layer. Compared with the previous studies, not only the bridge foundation but also the bridge superstructure is modeled. In this paper, the seismic behavior of pile-supported bridge abutments located on soft clay layers with different materials and thicknesses is reported.

2. Experimental program

2.1 Experimental parameters

In the dynamic centrifuge experiment, the pile-supported bridge abutment at the movable bearing side is modeled. The experimental scale is set to 1/75 considering the centrifuge loading device capacity. As shown in Table 1, to investigate the effect of the lateral movement of the soft clay layer on the seismic behavior of the bridge abutment, three cases are designed with different thicknesses and materials of the soft clay layer. In Case 1, designated as the basic case, the soft clay layer has 160 mm thickness at the model scale and is made of kaolin clay material. Case 2 has a soft clay layer with the same thickness as Case 1 but is made of



sumi clay material. Case 3 has a soft clay layer made of kaolin clay material but with a 240 mm thickness larger than that of Case 1. The material properties of kaolin and sumi clay are shown in Table 2. The consolidation test results show that the sumi clay material has a larger consolidation yield stress than kaolin clay. Furthermore, the results of the consolidated-drained triaxial compression test show that the sumi clay also has larger shear strength.

Except for the soft clay layer, the three cases have the same thickness of the backfill layer and the bearing layer. Silica sand with a mean particle size equal to 0.29 mm is used to make these two layers. The relative densities of the backfill layer and the bearing layer are 80% and 90%, respectively. The three cases also have the same pile conditions. The pile foundation is designed with the layout of a 3×4 pile group, and the pile diameter is equal to 14 mm in the model scale.

The acceleration wave named 2-I-I-3, which is chosen from the acceleration wave database prescribed in the Design Specifications for Highway Bridges of Japan [11] for bridge dynamic numerical analysis, is adopted as the input earthquake motion, considering the similarity law between the model and prototype. Due to the limitation of the loading device capacity, the acceleration amplitude is reduced to 80% in the centrifuge experiment. The input acceleration wave is shown afterwards, along with other ground acceleration responses.

Table 1 – Experimental parameter setting (model scale)

Case	ground conditions						pile conditions	
	backfill layer		soft clay layer		bearing layer		pile group	diameter
	thickness	material	thickness	material	thickness	material		
1	160 mm	silica sand	160 mm	kaolin clay	80 mm	silica sand	3×4	14 mm
2				sumi clay*				
3			240 mm	kaolin clay				

*One kind of mineral powder, made by Sumitomo Osaka Cement Co., Ltd., Japan.

Table 2 – Material properties of kaolin and sumi clay

	material	kaolin clay	sumi clay
consolidation test	compression index C_c	0.336	0.195
	consolidation yield stress (kN/m^2)	66.9	375.0
consolidated-drained triaxial compression test	cohesion c (kN/m^2)	13.3	46.1
	friction angle ϕ ($^\circ$)	9.2	16.7

2.2 Bridge abutment model

Figure 1 shows the schematic diagram of the bridge abutment model for Case 1, along with the surrounding ground set in the rigid soil container. Cases 2 and 3 have similar schematic diagrams of the bridge abutment model to Case 1. In addition to the bridge abutment model with the 3×4 pile group, the bridge abutments with the 3×2 pile group are also set at two sides to reduce the adhesion effect between the soil container wall and the soft clay soil. A sponge material is also installed between the central and side bridge abutment models to reduce the friction effect. To simulate the collision between the bridge abutment at the movable bearing side and the superstructure, the simply fabricated girder is set by fixing one end to the soil container wall. The spacing between the girder end and the bridge abutment wall is set equal to 1 mm at the model scale.

Figure 2 shows the details of the central bridge abutment for the three cases. The abutment wall model has dimensions of 140 mm \times 160 mm \times 15 mm (length \times height \times thickness), and the footing model has dimensions of 140 mm \times 105 mm \times 30 mm (length \times width \times thickness) in three directions. Both the abutment wall and the footing models are made of aluminum material.



The pile models shown in Figure 3 for the three cases are made of aluminum pipe with 14 mm outer diameter and 1 mm wall thickness. The material properties of the aluminum pipe are shown in Table 3. Three cases have different pile lengths. Cases 1 and 2 have the same pile length equal to 210 mm, which is measured from the footing bottom; Case 3 has a pile length equal to 290 mm. In all three cases, the pile head is rigidly fixed to the footing model; the lower end is inserted into the bearing layer with the embedment length equal to 50 mm. Additionally, the pipe spacing shown in Figure 2 is 35 mm in all three cases, which is equal to two and half times the pile diameter.

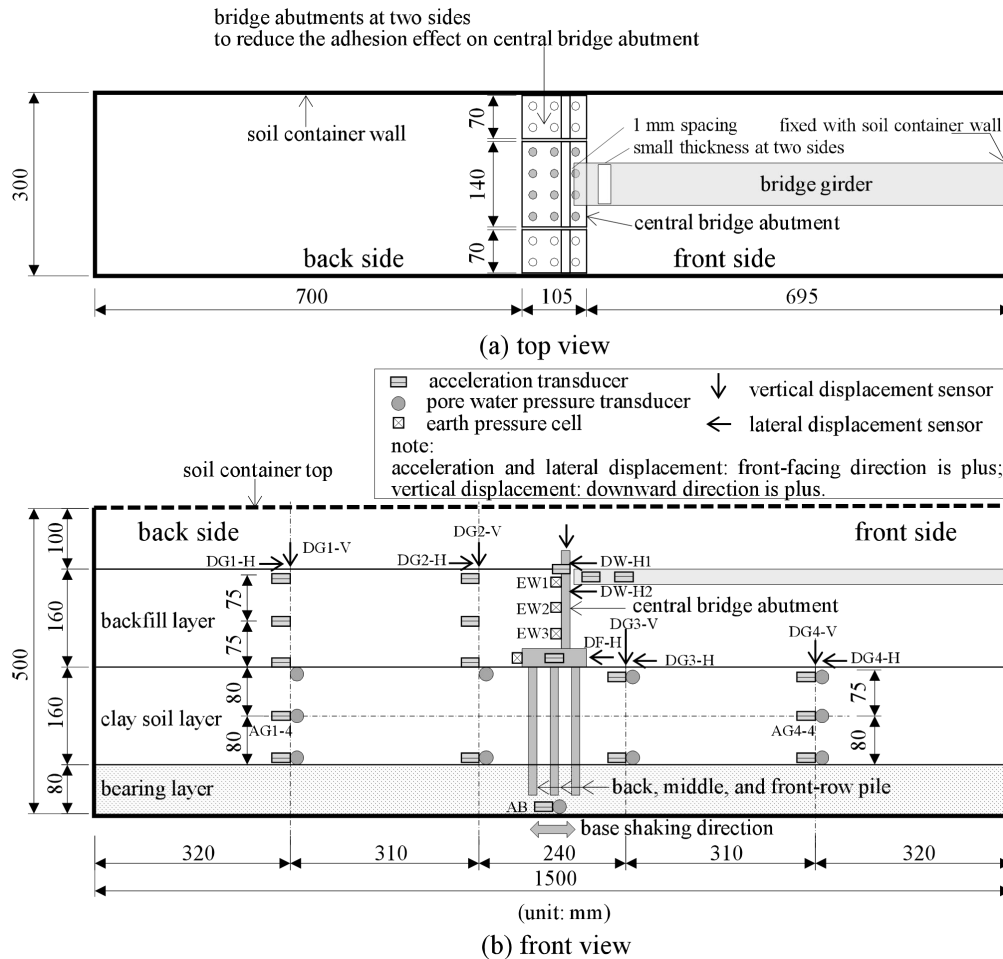


Fig. 1 – Schematic diagram of the bridge abutment model set in the soil container (Case 1)

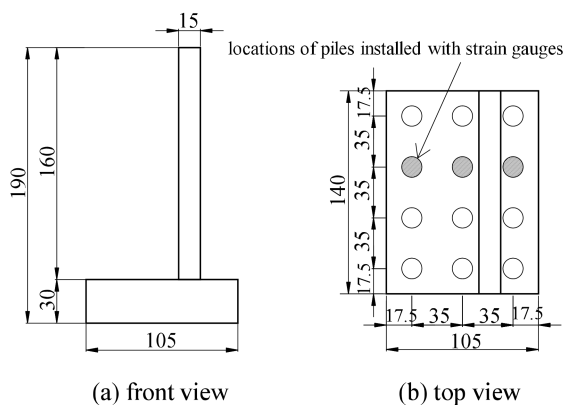


Fig. 2 – Details of the central bridge abutment model

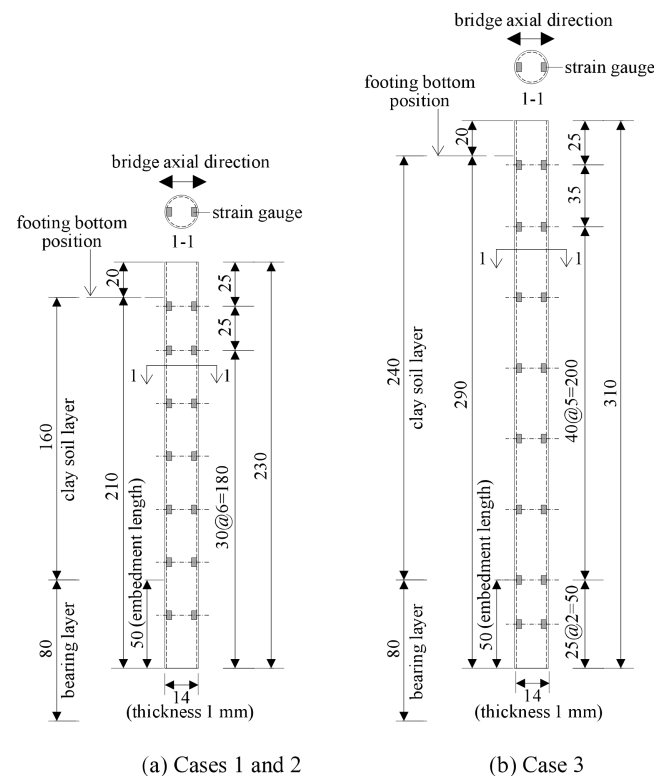


Fig. 3 – Details of the pile models

Table 3 –Material properties of aluminum pipe

tensile test	yielding strength* (N/mm ²)	yielding strain (μ)	Young's modulus (N/mm ²)
1	195.8	4879	69.7
2	195.2	4853	68.4
3	199.0	4853	69.5
average	196.7	4862	68.9

* yielding strength is obtained by the 0.2% offset strain method.

2.3 Experimental measurement

As shown in Figure 1, several types of transducers are placed at the bridge abutment model as well as the surrounding ground. These transducers include acceleration transducers, pore water pressure transducers, earth pressure cells, and displacement sensors. After the centrifuge experiment, the ground is also cut to investigate the residual displacement at different depths, by measuring the movement of the measurement mark buried in the ground.

In addition, strain measurements are also conducted for the bridge girder, the abutment wall, and the piles. The bridge girder model is made with a small thickness near the left end to accurately measure the axial strain and to evaluate the axial force due to the collision with the abutment wall. The bending strain at the base of the abutment wall is also measured to evaluate the base bending moment. To evaluate the bending moments acting on the pile sections, three piles shown in Figure 2 are chosen to install strain gauges for each case, and the strain gauge arrangement is shown in Figure 3. The strain gauges are placed at the inner surface of the pile models. Cases 1 and 2 have seven sections, and Case 3 has eight sections installed with strain gauges.



2.4 Experimental procedure

In this centrifuge experiment, the manufacturing sequence of the ground model and the installation sequence of the bridge abutment model are explained as follows. First, the bearing layer is made at the bottom of the soil container. Second, the soft clay slurry is put into the soil container after the placement of the pile model; then, the soft clay slurry is consolidated with the overburden load at the 75 g field. Third, after 90% consolidation of the soft clay layer is finished, the consolidated soft clay layer is cut down to the designed thickness at the 1 g field; then, the installation of the footing and the abutment wall model is conducted, and the backfill layer is made. Fourth, after the girder is set, the completed ground model installed with the bridge abutment model is consolidated again at the 75 g field until 90% consolidation is reached.

After 90% consolidation of the soft clay layer is completed, the spacing between the girder and the abutment wall model is adjusted to approximately 1 mm at the 1 g field; then, at the 75 g field, base shaking in the longitudinal direction of the soil container is conducted under the undrained condition. With regard to the experimental data collection during the base shaking phase, the initial zero points of these transducers are set at the beginning of the second time of the clay soil consolidation, not the beginning of the base shaking phase.

Note that in the following sections, to easily understand the seismic behavior of the bridge abutment subjected to the lateral movement of the soft clay layer, the experimental results are shown and illustrated at the prototype scale.

3. Experimental results and discussions of the ground behavior

3.1 Acceleration response

The acceleration response of the soft clay layer is mainly explained. Three cases have similar experimental results. The measured time histories of the acceleration response (AG1-4 and AG4-4) at the middle depth of the soft clay layer of Case 1, along with the input earthquake motion (AB) measured at the soil container bottom, are shown in Figure 4 as an example. In the soft clay layer at the back side of the abutment wall, the acceleration amplification phenomenon is observed over the whole shaking time period. However, in the soft clay layer at the front side, the acceleration amplification phenomenon is only observed approximately before 75 s; after 75 s, the acceleration attenuation obviously occurs. The reason can be explained by the rigidity degradation of clay soil due to cyclic shearing during base shaking. In particular, for the soft clay layer at the front side, due to the small effect restraint pressure, the cyclic shearing effect on the rigidity degradation is more remarkable.

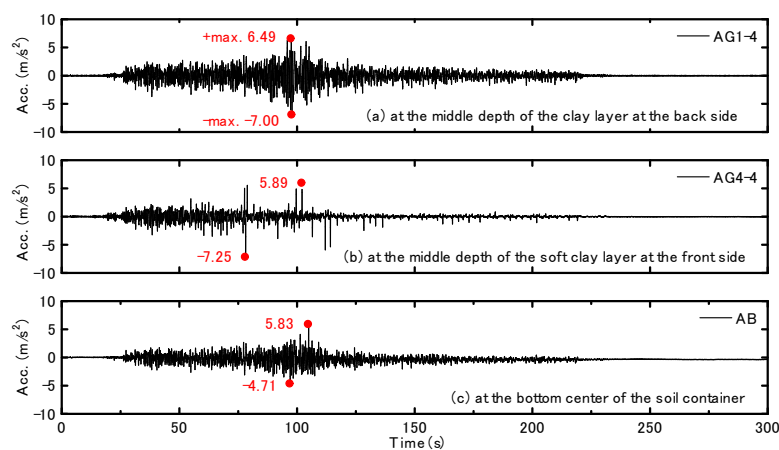


Fig. 4 – Time histories of the acceleration response (Case 1)



3.2 Displacement response

The measured lateral displacement and settlement at the ground surface in Case 1 are shown in Figure 5(a) and (b), respectively. For the experimental results at the beginning of the base shaking phase (0 s), which shows the lateral displacement and the settlement caused by the clay soil consolidation before base shaking, there is no obvious difference between the lateral displacements at points DG1 to DG4; however, due to the different overburden loads of the soft clay layer on the two sides, the settlements (DG1-V and DG2-V) on the back side are apparently larger than those on the front side. During the base shaking time from 50 to 150 s, the lateral displacement and the settlement obviously increase, except for the settlement (DG3-V and DG4-V) at the front side. In particular, the lateral displacement (DG3-H) near the abutment wall at the front side and the settlement (DG2-V) near the abutment wall at the back side largely increase. At the end of the base shaking phase of approximately 300 s, both the residual lateral displacement and settlement are almost equal to their maximum values during base shaking. With regard to the change tendency and the magnitude relation of the lateral displacements and the settlements, Cases 2 and 3 have similar results to Case 1.

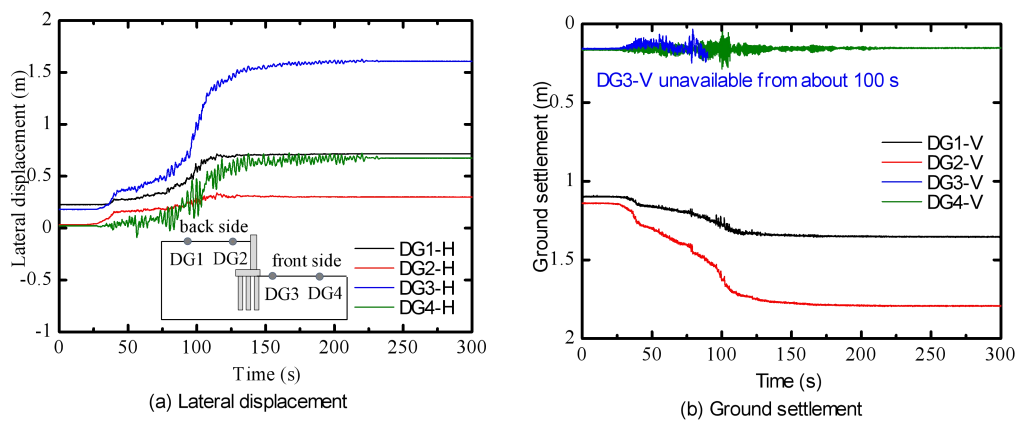


Fig. 5 – Time histories of the lateral displacement and settlement at the ground surface (Case 1)

4. Experimental results and discussions of the bridge abutment behavior

4.1 Lateral displacement response

Figure 6 shows the time histories of the lateral displacement at different heights of the bridge abutment wall in Case 1. At the beginning of the base shaking phase (0 s), the lateral displacement at the top (DW-H1) is larger than that at the footing location (DF-H), showing that the bridge abutment wall has inclined forward due to the consolidation effect. From the base shaking time of approximately 50 s, the lateral displacement at the footing location (DF-H) is larger than that at the abutment wall top (DW-H1), showing the inverse magnitude relation of the lateral displacements. That is, the bridge abutment wall inclines backward during base shaking. It is because that the abutment wall is restrained at the top due to the collision with the bridge girder; however, since the pile foundation is subjected to the lateral movement of the soft clay layer, the lateral displacement at the footing location sharply increases. Cases 2 and 3 have similar results to Case 1 regarding the lateral displacement of the bridge abutment.

4.2 Rotation response

Based on the lateral displacements DW-H1 and DW-H2, the rotation angle of the bridge abutment is evaluated and shown in Figure 7 for the three cases. At the beginning of the base shaking phase (0 s), Case 2 exhibits a slight forward inclination that is equal to Case 1; however, due to the high shear strength of the clay soil, the change in the rotation angle during the base shaking phase in Case 2 is obviously smaller than

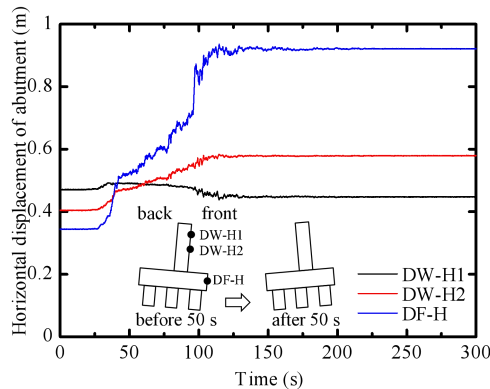


Fig. 6 – Lateral displacement of the bridge abutment (Case 1)

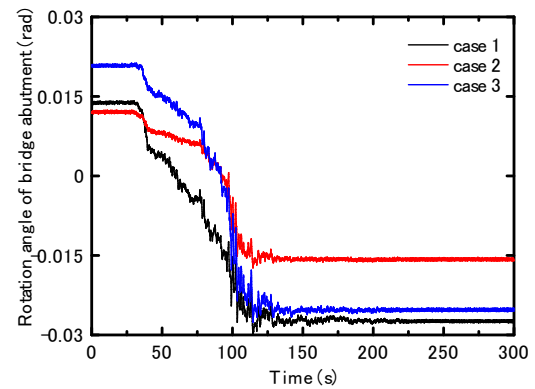


Fig. 7 – Rotation angle of the bridge abutment (Case 1)

that of Case 1. Although Case 3 exhibits a larger forward inclination than Case 1 at the beginning of the base shaking phase, their maximum backward inclination angles during base shaking are almost identical to each other; a larger change in the rotation angle is demonstrated in Case 3 during the base shaking phase. In all three cases, the residual rotation angles are almost equal to their maximum value during the base shaking phase.

4.3 Pile bending moment distribution

The pile bending moment distributions, which are evaluated based on the measured axial strain, are shown in Figure 8 for the three cases.

By comparing the bending moments at the beginning of the base shaking phase (0 s) and at the maximum response point during the base shaking, the bending moment in the three cases largely increases when subjected to the base shaking-induced lateral movement of the soft clay layer. In addition, the results of the three cases similarly show that the bending moment largely remains even at the end of the base shaking phase (299.9925 s) compared with their maximum response.

At the maximum response point, the bending moment of the back-row pile in each case is larger than that of the middle and front-row piles. Furthermore, the second derivative result (i.e., curve curvature) of the pile bending moment distribution curve can be considered corresponding to the external pile earth pressure. As shown in Figure 8, the curvature of the bending moment distribution curve of the back-row pile in each case is larger than that of the middle and front-row piles. In other words, under the lateral movement of the soft clay layer, the back-row pile suffers a larger earth pressure than the middle and front-row piles.

Although the ground displacement and the abutment rotation angle in Case 2 are obviously smaller than those in Case 1, Figure 8(a) and (b) show that Case 2 does not have a clear tendency of the pile bending moment to be smaller than that in Case 1 at the maximum response point. This effect can be explained from the aspect of the pile earth pressure magnitude. The curvature of the pile bending moment distribution curve of Case 2, especially of the back-row pile, is clearly larger than that of Case 1, showing the larger pile earth pressure in Case 2. In other words, for the pile-supported bridge abutment constructed on the soft clay layer with a high shear strength, the lateral movement of the soft clay layer may induce a large external earth pressure on the piles during an earthquake.

Although the thickness of the soft clay layer in Case 3 is larger than that in the basic Case 1, Figure 8(a) and (c) show that the bending moments near the pile head in the two cases are generally equal to each other at the maximum response point. This result can also be explained from the aspect of the pile earth pressure magnitude. The bending moment distribution indicates that the larger earth pressure in Case 3 is only limited to the back-row pile at a depth of approximately 6 m, instead of the whole pile length. In other words, for a pile-supported bridge abutment constructed on a soft clay layer with a large thickness, a large

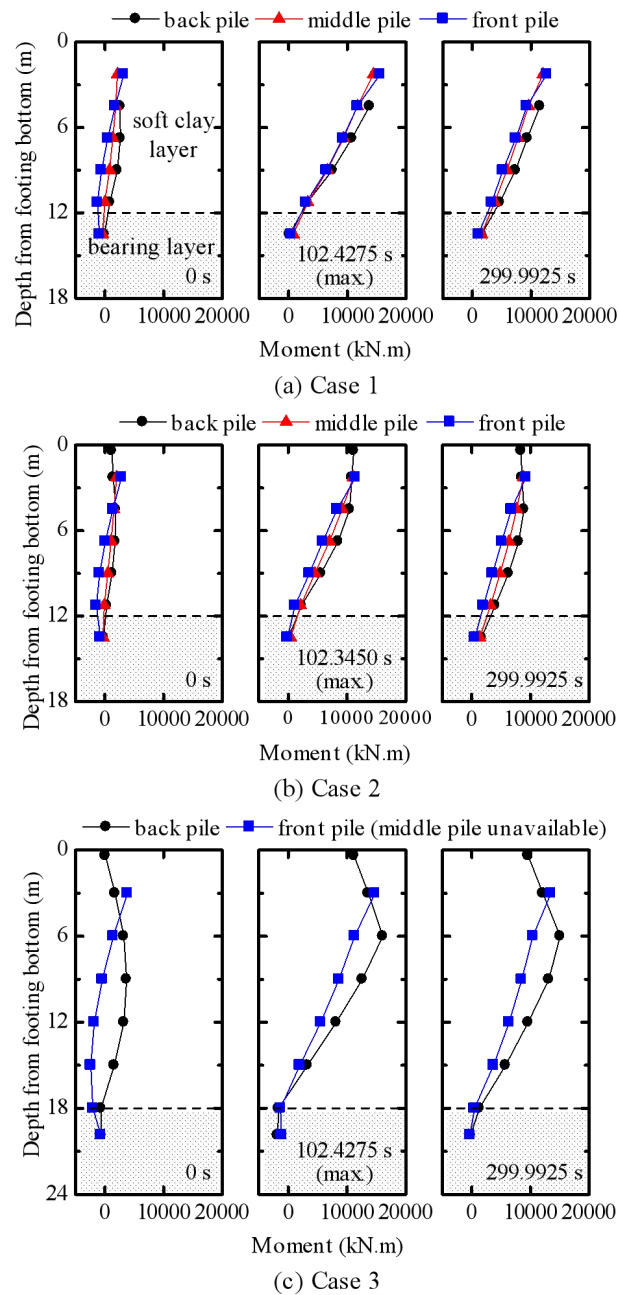


Fig. 8 –Pile bending moment distributions

earth pressure may occur at the local position of the piles during an earthquake, rather than the whole pile length.

5. Conclusions

To investigate the bridge seismic behavior subjected to the earthquake-induced lateral movement of the soft clay layer, the pile-supported bridge abutments located on the soft clay deposits with different materials and thicknesses at the movable bearing side is modeled, and the dynamic centrifuge experiments are conducted at a 75 g field. Based on the experimental results, the following major conclusions are obtained:



- (1) Under the effect of the earthquake-induced lateral movement of the soft clay layer, both the settlement at the back-side ground surface and the lateral displacement at the front-side ground surface near the bridge abutment wall are obviously larger than other locations.
- (2) The bridge abutment wall is restrained at the top position due to the collision with the girder; however, due to the lateral movement of the soft clay layer, the footing largely moves forward, resulting in a large backward inclination of the bridge abutment. Furthermore, it is confirmed that the shear strength and the thickness of the soft clay layer can largely affect the rotation angle of the bridge abutment.
- (3) It is found that due to the lateral movement of the soft clay layer, the pile bending moment largely increases during base shaking and largely remains even at the end of base shaking. It is also confirmed that the bending moment acting on the back-row pile is larger than that acting on the middle and front-row piles.
- (4) In the case that the material of the soft clay layer has a high shear strength, the ground lateral movement possibly causes a large external earth pressure on the piles, although the ground displacement is relatively small. Furthermore, due to the ununiform ground lateral movement at different depths, especially for the soft clay layer with a large thickness, the pile earth pressure may largely occur at the limited scope of the piles, rather than the whole pile length.

6. References

- [1] Public Works Research Institute (2014) Reconnaissance report on damage to road bridges by the 2011 Great East Japan Earthquake. Technical Note, No. 4295. Tsukuba, Japan: PWRI (in Japanese).
- [2] Chandrasekaran SS, Boominathan A, Dodagoudar GR (2010). Experimental investigations on the behaviour of pile groups in clay under lateral cyclic loading. *Geotechnical and Geological Engineering*, 28(5): 603-617.
- [3] Banerjee S, Goh SH, Lee FH (2014) Earthquake-induced bending moment in fixed-head piles in soft clay. *Géotechnique*, 64(6): 431-446.
- [4] Wilson DW, Boulanger RW, Kutter BL (1997) Soil-pile-superstructure Interaction at soft or liquefiable soil sites: centrifuge data report for CSP4. Center for Geotechnical Modeling, Department of Civil and Environmental Engineering.
- [5] Wilson DW (1998) Soil-pile-superstructure interaction in liquefying sand and soft clay. Doctoral dissertation, University of California, Davis.
- [6] Zhang L, Goh SH, Yi J (2017) A centrifuge study of the seismic response of pile-raft systems embedded in soft clay. *Géotechnique*, 67(6): 479-490.
- [7] Garala, TK, Madabhushi, GS (2019) Seismic behaviour of soft clay and its influence on the response of friction pile foundations. *Bulletin of Earthquake Engineering*, 17(4): 1919-1939.
- [8] Boominathan A, Ayothiraman R (2006) Dynamic response of laterally loaded piles in clay. *Proceedings of the Institution of Civil Engineers-Geotechnical Engineering*, 159(3): 233-241.
- [9] Yang J, Yang, M, Chen H (2019) Influence of pile spacing on seismic response of piled raft in soft clay: centrifuge modeling. *Earthquake Engineering and Engineering Vibration*, 18(4): 719-733.
- [10] Qiu Z, Ebeido A, Almutairi A, et al. (2020) Aspects of bridge-ground seismic response and liquefaction-induced deformations. *Earthquake Engineering & Structural Dynamics*. DOI: 10.1002/eqe.3244.
- [11] Japan Road Association (2017) Design specifications of highway bridges. Tokyo, Japan: JRA (in Japanese).